

A Multicolor Cationic Conjugated Polymer for Naked-Eye Detection and Quantification of Heparin

Kan-Yi Pu and Bin Liu*

Department of Chemical and Biomolecular Engineering, 4 Engineering Drive 4, National University of Singapore, Singapore 117567, Singapore

Received June 6, 2008; Revised Manuscript Received July 16, 2008

ABSTRACT: A new cationic polyfluorene derivative with 20 mol % 2,1,3-benzothiadiazole (BT) content was synthesized via Suzuki cross-coupling polymerization. The high charge density and cationic oligo(ethylene oxide) side chains endue the polymer with a good water solubility (~ 12 mg/mL), leading to a low inherent BT emission background in buffer. Addition of negatively charged heparin into the polymer solution induces polymer aggregation, giving rise to enhanced energy transfer from the fluorene segments to the BT units. With increasing heparin concentrations, the orange BT emission intensity progressively increases at the expense of the blue fluorene emission. In contrast, addition of hyaluronic acid, an analogue of heparin, results in an insignificant enhancement in BT emission. This selective optical signature not only allows distinguishing heparin from hyaluronic acid but also highlights the importance of electrostatic attraction between the polymer and the analyte in an energy transfer process. Heparin quantification is demonstrated by the linear intensity increase in the BT emission as a function of heparin concentration, providing a practical calibration scope ranging from 30 nM to 48 μ M. Moreover, the distinguishable solution fluorescent color at different heparin concentrations makes naked-eye heparin detection and quantification feasible. This study hence reports a general approach to construct convenient multicolor biosensors using cationic conjugated polymers with energy donor–acceptor architecture.

Introduction

Heparin is a naturally occurring sulfated polysaccharide belonging to the category of glycosaminoglycans.¹ Because of its interaction with diverse proteins, heparin plays a significant role in the regulation of various physiological processes, such as cell growth and differentiation, inflammatory process, and blood coagulation process.^{1a} Heparin has been widely employed as a major clinical anticoagulant drug to prevent thrombosis during surgery and to treat thrombotic diseases.² This clinical application of heparin is based on its unique capability of accelerating the rate at which antithrombin inhibits serine proteases in the blood coagulation cascade.² However, heparin overdose could induce thrombocytopenia, which is recognized as one of the most catastrophic complications of heparin treatment.³ Close monitoring and quantification of heparin is of vital importance not only for its regulation in the physiological process but also for its clinical application during surgery and postoperative therapy period.

Traditional clinical procedures for heparin quantification rely on the measurement of activated clotting time (ACT)⁴ or activated partial thromboplastin time (aPTT).⁵ These indirect methods are not sufficiently reliable, accurate, and amenable to clinical settings.⁶ Recently, fluorescent assays for heparin quantification have been reported, which employed synthetic cationic chromophores or chromophore-tethered flexible copolymers as heparin receptor.⁷ These assays adopt fluorescence quenching as signal output, which is undesirable for heparin quantification and visual detection. More recently, a peptide-based sensor was reported to show fluorescence increase upon interaction with heparin.⁸ However, the detection window of the fluorescence turn-on sensor (0–0.06 U/mL) is out of the clinical range (0.2–8 U/mL). Development of effective and visual fluorescent assays for heparin quantification is in urgent demand, which becomes a challenge in the field of chemical and biological sensors.

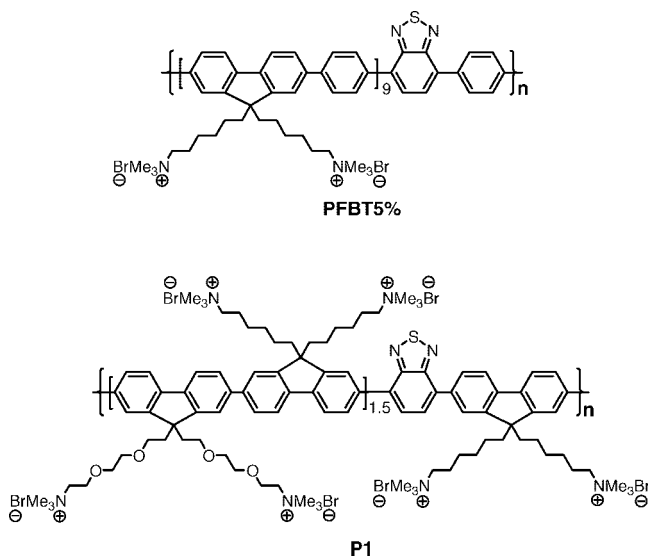
A unique platform for construction of chemical and biological sensors has been provided by conjugated polyelectrolytes (CPEs)

which combine the optoelectronic properties of π -conjugated polymers with water solubility of polyelectrolyte.⁹ In comparison with small molecular counterparts, the delocalized electronic backbone structure of CPEs allows more rapid intrachain and interchain energy transfer.¹⁰ In particular, interchain fluorescence resonance energy transfer (FRET) was reported to be more efficient than intrachain FRET due to stronger electronic coupling and increased transfer dimensionality for interchain vs intrachain interactions.¹¹ According to this mechanism, a cationic poly(fluorene-*alt*-1,4-phenylene) derivative containing 5 mol % 2,1,3-benzothiadiazole (BT) units (**PFBT5%**) was developed for multicolor sensing.¹² In dilute solutions, the polymer emits blue. Complex formation between the polymer and oppositely charged DNA molecules induces polymer aggregation and increases the local concentration of BT units, leading to enhanced interchain contacts and improved electronic coupling between optical partners. Under these conditions, energy transfer between the fluorene–phenylene fragments (donor) and the BT units (acceptor) is more efficient than that for isolated chains, and thus green emission dominates the solution fluorescence. The aggregation-induced blue-to-green fluorescence change was subsequently implemented for DNA quantification.¹³ Recently, an anionic poly(*p*-phenylene ethynylene) (PPE) comprising low-energy traps was also reported to detect cationic amines.¹⁴ To improve the sensitivity and broaden the quantification range of these assays, the main challenge is to synthesize donor–acceptor CPEs with good water solubility and high acceptor content.

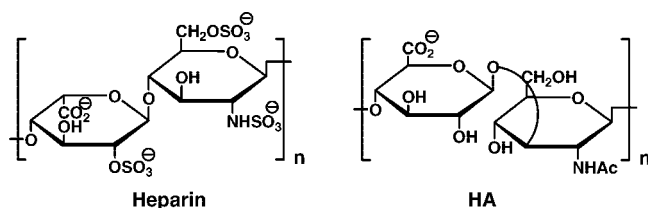
In this contribution, we design and synthesize a new BT-containing cationic conjugated polymer (CCP) with high water solubility and 20 mol % BT content (**P1**). The chemical structure of **P1** is shown in Scheme 1 along with **PFBT5%**. The optical properties of **P1** are investigated and compared with **PFBT5%** to demonstrate the side-chain modification in improving water solubility and its effect on the intrinsic BT emission prior to analyte addition. The negatively charged sulfated groups of heparin enable the complexation with the polymer via electrostatic attractions. As such, a multicolor biosensor for heparin detection and quantification can be developed by taking

* Corresponding author. E-mail: cheliub@nus.edu.sg.

Scheme 1. Chemical Structures of PFBT5% and P1



Scheme 2. Chemical Structures of Heparin and HA

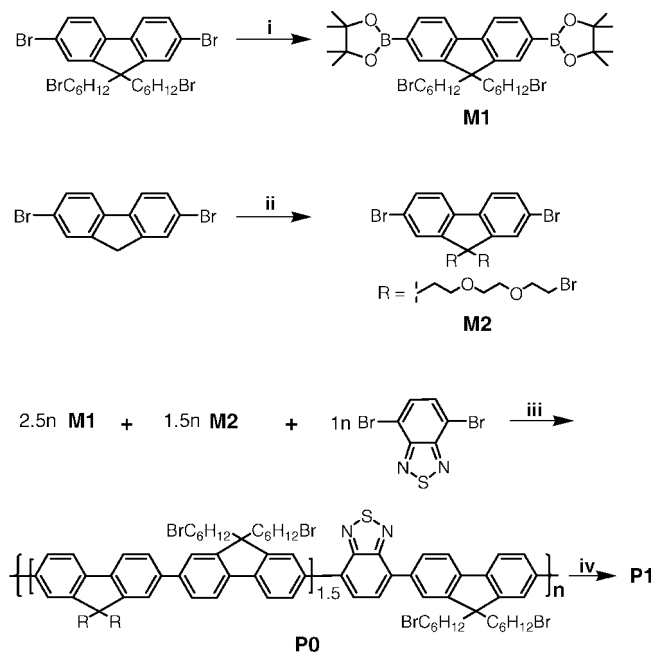


advantage of the polymer/heparin complex formation to induce FRET from the fluorene fragments to the BT units. Moreover, the optical response of **P1** to heparin and its analogue hyaluronic acid (HA) is compared to probe the effect of electrostatic attraction on FRET. The chemical structures of heparin and HA are shown in Scheme 2. In addition to these investigations, we also show that **P1** can be utilized for naked-eye detection and quantification of heparin with the assistance of a hand-held UV lamp.

Results and Discussion

Synthesis and Characterization. CCPs with high BT content are desirable since they offer high sensitivity for analyte detection.¹⁵ However, high BT content polymers were found to show undesired BT emission in aqueous solution prior to analyte addition.^{13b} Synthetic efforts are thus focused on the optimization of polymer structure in order to obtain a CCP with high BT content as well as good water solubility.

Scheme 3 depicts the synthetic approach toward **P1**. The dioxaborolane monomer, 2,7-bis[9,9'-bis(6''-bromohexyl)fluorenyl]-4,4,5,5-tetramethyl[1.3.2]dioxaborolane (**M1**), was synthesized in 59% yield by heating a mixture of 2,7-dibromo-9,9'-bis(6-bromohexyl)fluorene and bis(pinacolato)diborane with KOAc in dioxane at 85 °C for 12 h. In a two-phase basic deprotonation condition, 2,7-dibromofluorene was alkylated with 1,2-bis(2-bromoethoxy)ethane to afford 2,7-dibromo-9,9'-bis(2-(2-bromoethoxy)ethoxy)ethyl)fluorene (**M2**) in 48% yield. The correct structures of **M1** and **M2** were affirmed by NMR, elemental analysis, and mass spectrometry. The Suzuki cross-coupling-mediated copolymerization of **M1**, **M2**, and 4,7-dibromo-2,1,3-benzothiadiazole at a feed ratio of 0.5:0.3:0.2 provided the neutral statistical random copolymer (**P0**). The number-average molecular weight and polydispersity of **P0** are 11 000 and 3.0, respectively, determined by GPC using THF as the solvent and polystyrene as

Scheme 3. Synthetic Route of P1^a

^a Reagents and conditions: (i) bis(pinacolato)diborane, [Pd(dppf)Cl₂], KOAc, dioxane, 85 °C, 12 h; (ii) 1,2-bis(2-bromoethoxy)ethane, TBAB, KOH/H₂O, 75 °C, 15 min; (iii) [Pd(PPh₃)₄], K₂CO₃, toluene/H₂O, 90 °C, 24 h; (iv) THF/H₂O, NMe₃, 24 h.

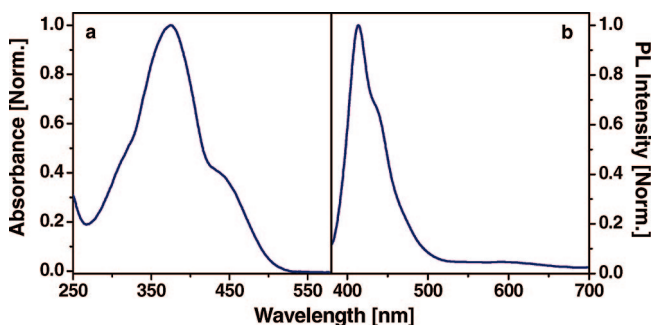


Figure 1. Normalized absorption (a) and PL spectra (b) of **P1** at [RU] = 3 μ M in water (excitation at 365 nm).

the standard. Further treatment of **P0** with trimethylamine in THF/water yielded the BT-containing CCP (**P1**). The chemical structures of **P0** and **P1** were determined by ¹H and ¹³C NMR spectroscopies. According to the ¹H NMR spectrum of **P0**, the ratio of the integrated area of the signal at 3.68 ppm (−OCH₂CH₂Br from **M2**) to that of the signal at 2.18 ppm (−CH₂(CH₂)₅Br from **M1**) is identical to 0.60. This indicates that the BT content in the polymer is the same as the feed ratio (20%), which is further affirmed by the elemental analysis of **P0**. The ratio of the integrated areas for −CH₂CH₂X (X = Br, N(CH₃)₃), and −CH₂CH₂N(CH₃)₃ in the ¹H NMR spectra of **P1** shows that the degree of quaternization is higher than 95%. **P1** is soluble in a variety of polar solvents, including dimethylformamide, dimethyl sulfoxide, methanol, and water. Noteworthy is that the water solubility of **P1** is ~12 mg/mL at 24 ± 1 °C. The high water solubility of **P1** results from the high charge density and the oligo(ethylene oxide) side chains.¹⁶

Optical Properties. The UV–vis absorption and photoluminescence (PL) spectra of **P1** in water are depicted in Figure 1. The concentration of **P1** based on repeat unit ([RU]) is 3 μ M.¹⁷ The absorption spectrum of **P1** exhibits a maximum at 375 nm corresponding to the fluorene segments and a characteristic band ranging from 426 to 520 nm corresponding to the

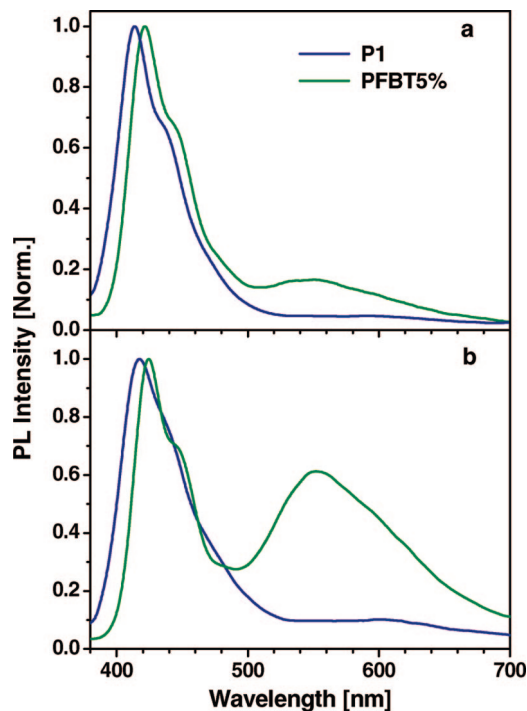


Figure 2. Normalized PL spectra of **P1** and **PFBT5%** at $[RU] = 3 \mu\text{M}$ (a) and $[RU] = 60 \mu\text{M}$ (b) in 2 mM PBS buffer at pH = 7.4 (excitation at 365 nm).

BT units.¹³ The emission spectrum of **P1** shows a maximum at 415 nm with almost no obvious emission band in 500–650 nm region as an indication of inefficient FRET in dilute solution.¹³

Figure 2 shows the normalized PL spectra of **P1** and **PFBT5%** with $[RU] = 3$ or $60 \mu\text{M}$ in 2 mM phosphate–buffer saline (PBS at pH = 7.4) upon excitation at 365 nm. For **PFBT5%**, the BT emission band ranging from 500 to 650 nm is visible at both concentrations. The higher ratio of the green/blue emission intensity at $[RU] = 60 \mu\text{M}$ as compared to that at $[RU] = 3 \mu\text{M}$ indicates that aggregation of **PFBT5%** occurs at elevated concentrations due to its poor water solubility.^{14a} On the contrary, the PL spectra of **P1** is dominated by the blue emission, and the BT emission is weak at $[RU] = 3$ and $60 \mu\text{M}$. This originates from the high water solubility of **P1** that inhibits polymer aggregation. The difference in the concentration-dependent BT emission between **P1** and **PFBT5%** highlights the importance of polymer structural design, which makes **P1** more suitable for heparin detection and quantification than **PFBT5%** does.

Aggregation-Induced FRET. Heparin titration experiments were conducted at $[RU] = 60 \mu\text{M}$ in 2 mM PBS (pH = 7.4). The heparin concentration was calculated using sugar dimer as the repeat unit. Figure 3a shows the changes in the PL spectra of **P1** upon addition of heparin from 0 to $50 \mu\text{M}$ at intervals of $2 \mu\text{M}$. As $[\text{heparin}]$ increases, the orange emission band at 595 nm progressively grows at the expense of the blue emission band at 415 nm. An isosbestic point is observed at 515 nm. This transformation in the PL spectra of **P1** reflects gradually increased FRET from the fluorene segments (energy donor) to the BT units (energy acceptor) upon **P1**/heparin complex formation. At $[\text{heparin}] = 48 \mu\text{M}$, the intensity of the orange emission band reaches its maximum, indicating the analyte-receptor saturation. At this point, the concentration of negative charges from heparin is $192 \mu\text{M}$, while the concentration of positive charges from **P1** is $190 \mu\text{M}$. The nearly identical concentration of opposite charges at saturation is consistent with the previous reports that charge balance is essential for complexation between oppositely charged polymers and analytes based on electrostatic interactions.^{12,13}

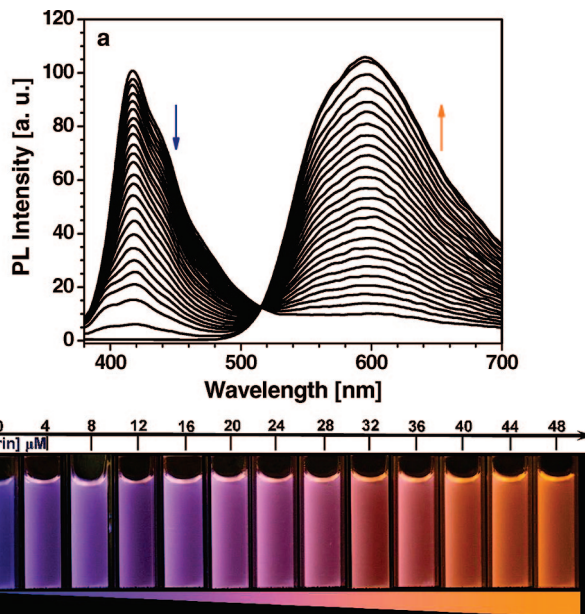


Figure 3. (a) PL spectra of **P1** at $[RU] = 60 \mu\text{M}$ in 2 mM PBS at pH = 7.4 in the presence of heparin with concentrations ranging from 0 to $50 \mu\text{M}$ at intervals of $2 \mu\text{M}$ (excitation at 365 nm). (b) Changes in the fluorescent color of the corresponding solution at intervals of $4 \mu\text{M}$ under a hand-held UV lamp with $\lambda_{\text{max}} = 365 \text{ nm}$.

Changes in the PL spectra of polymer solution could be monitored by naked-eye under a portable UV lamp with $\lambda_{\text{max}} = 365 \text{ nm}$. Figure 3b shows heparin-induced solution fluorescence change with $[\text{heparin}] = 0\text{--}48 \mu\text{M}$ at intervals of $4 \mu\text{M}$. The color of solution fluorescence gradually transfers from blue to orange with increasing $[\text{heparin}]$. At the low $[\text{heparin}]$ range ($0\text{--}16 \mu\text{M}$), the solution fluorescent color appears blue; at the moderate $[\text{heparin}]$ range ($20\text{--}28 \mu\text{M}$), the solution fluorescent color appears pink; and at the high $[\text{heparin}]$ range ($>28 \mu\text{M}$), the solution fluorescent color appears orange. The distinguishable color at different heparin concentrations should benefit from the similar rate of countercurrent fluorescence changes in the fluorene emission band at 415 nm and the BT emission band at 595 nm. As a result, naked-eye quantification of heparin is feasible using the CCP-based heparin assay. Since the therapeutic dosing level of heparin ranges from 0.2 to 8 U/mL (1.8 to $72 \mu\text{M}$), depending on the clinical treatment,¹⁸ the range of heparin concentration obtained by this assay ($0\text{--}48 \mu\text{M}$) is practical.

To understand the importance of electrostatic attraction in the heparin-induced BT emission, similar experiments were performed with HA, an analogue of heparin. Heparin has four negatively charged side groups per repeat unit, while HA possesses only one negatively charged group per repeat unit (shown in Scheme 2), implying a weaker electrostatic attraction between HA and **P1** than that between heparin and **P1**. Upon addition of HA into the **P1** solution at $[RU] = 60 \mu\text{M}$ in 2 mM PBS, very small variations in the PL spectra of **P1** are observed. The normalized PL spectra of **P1** at $[\text{heparin}]$ or $[\text{HA}] = 44 \mu\text{M}$ are shown in Figure 4. A 110-fold higher intensity of the orange emission band in the presence of heparin to that in the presence of HA is observed, indicating the highly preferred response of **P1** to heparin over HA. This selectivity is associated with much stronger electrostatic attraction between heparin and **P1** in contrast to that between HA and **P1**, which consequently induces more compact polymer aggregation in the presence of heparin.¹⁶ Noteworthy is that within the tested $[\text{HA}]$ range the fluorescent color of **P1**/HA mixture remains blue, affording a facile way to distinguish heparin from HA by naked eye as demonstrated in the inset of Figure 4.

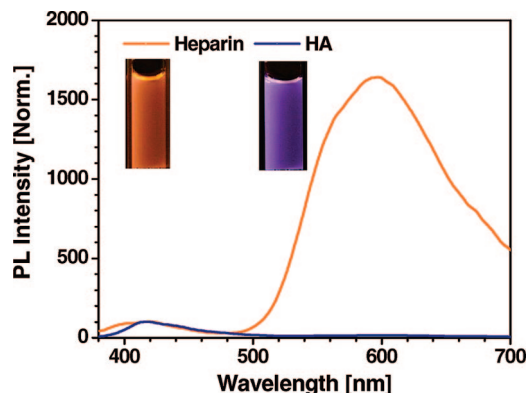


Figure 4. Normalized PL spectra of P1 at [RU] = 60 μM in the presence of [heparin] or [HA] = 44 μM in 2 mM PBS at pH = 7.4 (excitation at 365 nm). The inset shows the corresponding fluorescent color under a hand-held UV lamp with $\lambda_{\text{max}} = 365$ nm.

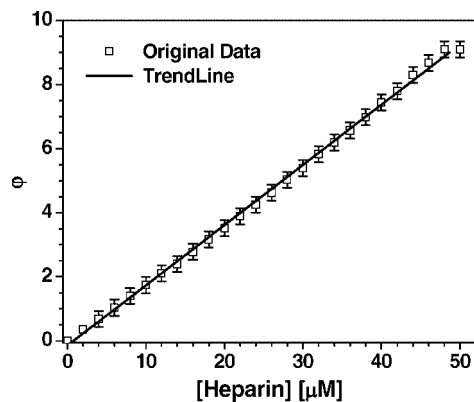


Figure 5. ϕ as a function of [heparin] and its linear trendline at [RU] = 60 μM in 2 mM PBS at pH = 7.4. The data are based on the average of three independent experiments.

Heparin Quantification. To demonstrate heparin quantification using the CCP-based assay, changes in the PL spectra of P1 in Figure 3a are correlated to [heparin]. To eliminate the discrepancy across different instruments and optical collection conditions, ϕ was defined as

$$\phi = (I - I_0)/I_0 \quad (1)$$

where I and I_0 are the intensities at 595 nm in the presence and absence of heparin, respectively. Figure 5 shows ϕ as a function of [heparin] together with its linear trendline, which has a slope of 0.19 μM^{-1} . The well overlap between the original data and the linear trendline in the range of 0–48 μM proves the validity of heparin concentration calibration using the CCP-based assay. The departure from the linear trendline at [heparin] > 48 μM is caused by receptor saturation as aforementioned. This indicates the upper detection limit for heparin is 48 μM using a P1 solution with [RU] = 60 μM .

To examine the low detection limit of the optical response, experiments were carried out using a dilute P1 solution with [RU] = 3 μM in 2 mM PBS. As shown in Figure 6, with increasing [heparin] at intervals of 30 nM, a progressive emission intensity increase at 595 nm is observed. Figure 6 shows ϕ as a function of [heparin] together with its linear trendline. Reducing the interval [heparin] to 3 nM only leads to a slight intensity decrease at 415 nm with almost no emission intensity increase at 595 nm. Addition of heparin with concentrations at intervals of 3 nM to P1 at [RU] = 0.3 μM in 2 mM PBS also cannot bring in any intensity increase at 595 nm. These data indicate that further decreasing the concentration of P1 or heparin is unable to induce efficient FRET, owing to the

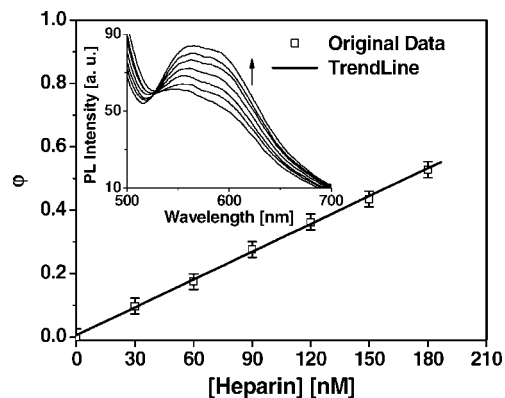


Figure 6. ϕ as a function of [heparin] and its linear trendline at [RU] = 3 μM in 2 mM PBS at pH = 7.4. The inset shows the corresponding PL spectra of P1 at [RU] = 3 μM in 2 mM PBS at pH = 7.4 upon addition of heparin with concentrations ranging from 0 to 180 nM at intervals of 30 nM. The data are based on the average of three independent experiments.

deficiency of polymer aggregation as compared to the assays operated at high concentrations. As a result, the low detection limit for the CCP-based assay for heparin quantification is close to [heparin] = 30 nM.

Conclusions

In summary, a multicolor biosensor for heparin detection and quantification was developed on the basis of the fluorescence change of a water-soluble BT-containing CCP. The operation mechanism takes advantage of strong electrostatic attraction between the CCP and heparin. Upon polymer/heparin complexation, orange emission is induced by FRET from the fluorene segments to the BT units in the aggregated state. Good affinity and selectivity of P1 for heparin over a similar polysaccharide (HA) lead to an obvious difference in the fluorescence change of P1, which can be easily distinguished by naked eye. The linear response of the orange-band emission vs heparin concentration allows efficient and accurate heparin quantification in a range of 30 nM (3.3 $\mu\text{g}/\text{mL}$) to 48 μM (~ 5 U/mL). In addition, adjustment of heparin quantification range for a specific application could be realized through varying polymer concentration. The most significant advantage of this assay is the feasibility of naked-eye detection and quantification of heparin in real time. The assay reported herein may find applications in research requiring rapid quantification of heparin in purified samples.

Experimental Section

Characterization. The NMR spectra were collected on a Bruker ACF400 (400 MHz). The element analysis was performed on Perkin-Elmer 2400 CHN/CHNS and Eurovector EA3000 elemental analyzers. GPC analysis was conducted with a Waters 2690 liquid chromatography system equipped with Waters 996 photodiode detector and Phenogel GPC columns, using polystyrenes as the standard and THF as the eluent at a flow rate of 1.0 mL/min at 35 $^{\circ}\text{C}$. UV-vis spectra were recorded on a Shimadzu UV-1700 spectrometer. Fluorescence measurements were carried out on a Perkin-Elmer LS-55 equipped with a xenon lamp excitation source and a Hamamatsu (Japan) 928 PMT, using 90 $^{\circ}$ angle detection for solution samples. Photographs of the polymer solutions were taken using a Canon EOS 400D digital camera under a hand-held UV lamp with $\lambda_{\text{max}} = 365$ nm. Fresh stock solutions for P1 (1 mM), HA (1 mM), and heparin (1 mM) were used. All the PL and UV experiments were carried out at 24 \pm 1 $^{\circ}\text{C}$. Milli-Q water (18.2 M Ω) was used for all the experiments.

Materials. All chemical reagents were purchased from Sigma-Aldrich Chemical Co. and were used as received. PFBT5%,¹² 2,7-dibromo-9,9'-bis(6-bromohexyl)fluorene,¹⁹ and 4,7-dibromo-2,1,3-

benzothiadiazole¹⁹ were synthesized according to our previous reports. 1,2-Bis(2-bromoethoxy)ethane were synthesized according to the literature.²⁰ Heparin molecular weight is determined by the common repeat dimer (644.2 g/mol). The heparin has 170 U/mg, and 1 μ M heparin corresponds to 0.11 U/mL.

2,7-Bis[9,9'-bis(6''-bromoethyl)fluorenyl]-4,4,5,5-tetramethyl-1,3,2-dioxaborolane (M1). 9,9'-Bis(bromoethyl)-2,7-dibromofluorene (6.5 g, 10 mmol), bis(pinacolato)diborane (6.0 g, 24 mmol), KOAc (7.0 g, 70 mmol), and dioxane (100 mL) were mixed together in a 250 mL flask. After degassing, [Pd(dppf)Cl₂] (0.5 g, dppf = 1,1'-bis(diphenylphosphanyl)ferrocene) was added. The reaction mixture was kept at 85 °C overnight and then cooled to room temperature. The organic solvent was distilled out, and the residual solid was dissolved in dichloromethane and washed with water. After drying with Na₂SO₄, the solvent was distilled out. The crude product was purified by flash chromatography using hexanes and dichloromethane (2:1) as the eluent to give **M1** as a white solid (4.2 g, 59%). ¹H NMR (400 MHz, CDCl₃, δ ppm): 7.86–7.77 (m, 2 H), 7.77–7.67 (m, 4 H), 3.25 (t, 4 H, *J* = 6.8 Hz), 2.08–1.93 (m, 4 H, *J* = 4.2 Hz), 1.64–1.57 (m, 4H, *J* = 7.2 Hz), 1.39 (s, 24 H), 1.17–1.13 (m, 4 H), 1.06–1.02 (m, 4 H), 0.54 (m, 4 H). ¹³C NMR (100 MHz, CDCl₃, δ ppm): 150.3, 144.1, 134.0, 128.9, 119.7, 84.0, 55.2, 40.1, 34.2, 32.8, 29.2, 27.9, 23.6. Element analysis calcd (%) for C₃₇H₅₄B₂Br₂O₄: C 59.71, H 7.31. Found: C 59.42, H 7.29. MS (EI): *m/z* 744.26 M⁺.

2,7-Dibromo-9,9'-bis(2-(2-(2-bromoethoxy)ethoxy)ethyl)fluorene (M2). 2,7-Dibromofluorene (1.23 g, 5 mmol) was added to a mixture of aqueous potassium hydroxide (100 mL, 50 wt %), tetrabutylammonium bromide (0.330 g, 1 mmol), and 1,2-bis(2-bromoethoxy)ethane (13.9 g, 50 mmol) at 75 °C. After 15 min, the mixture was cooled to room temperature. After extraction with CH₂Cl₂, the combined organic layers were washed successively with water, aqueous HCl (1 M), water, and brine and then dried over Na₂SO₄. After removal of the solvent and the excess 1,2-bis(2-bromoethoxy)ethane, the residue was purified by silica gel column chromatography using hexane and dichloromethane (1:2) as the eluent and recrystallized from ethanol and CH₂Cl₂ (5:1) to afford **M2** as white needle crystals (1.50 g, 48.0%). ¹H NMR (400 MHz, CDCl₃, δ ppm): 7.54–7.46 (m, 6 H), 3.68 (t, 4 H, *J* = 6.3 Hz), 3.39 (dd, 8 H, *J* = 4.4 Hz, *J* = 7.9 Hz), 3.20 (dd, 4 H, *J* = 3.6 Hz, *J* = 5.6 Hz), 2.80 (t, 4 H, *J* = 7.2 Hz), 2.34 (t, 4 H, *J* = 7.2 Hz). ¹³C NMR (100 MHz, CDCl₃, δ ppm): 150.95, 138.47, 130.69, 126.76, 121.64, 121.23, 71.15, 70.35, 70.04, 66.90, 51.97, 39.49, 30.90, 30.20. Element analysis calcd (%) for C₂₅H₃₀Br₂O₄: C 42.05 H 4.23. Found: C 42.06, H 4.31; MS (EI): *m/z* 713.89 (M⁺).

Synthesis of P0. **M1** (372 mg, 0.5 mmol), **M2** (240.67 mg, 0.3 mmol), 4,7-dibromo-2,1,3-benzothiadiazole (58.79 mg, 0.2 mmol), [Pd(PPh₃)₄] (5 mg), and potassium carbonate (828 mg, 6 mmol) were placed in a 25 mL round-bottomed flask. A mixture of water (3 mL) and toluene (5 mL) was added to the flask, and the reaction vessel was degassed. The mixture was vigorously stirred at 90 °C for 24 h and then precipitated into methanol. The polymer was filtered and washed with methanol and acetone and then dried under vacuum for 24 h to afford the neutral polymer **P0** (478 mg) as yellow fibers in 90% yield. ¹H NMR (400 MHz, CDCl₃, δ ppm): 8.13–7.55 (m, 10.4 H), 3.68 (t, 2.4 H, *J* = 6.1 Hz), 3.50–3.24 (m, 11.2 H), 3.21–2.71 (m, 2.4 H), 2.70–2.33 (m, 2.4 H), 2.30–2.00 (br, 4.0 H), 1.77–1.66 (br, 4.0 H), 1.33–1.16 (m, 8.0 H), 1.03–0.75 (br, 4.0 H). ¹³C NMR (100 MHz, CDCl₃, δ ppm): 154.35, 151.89, 151.54, 151.36, 151.01, 149.86, 149.38, 140.78, 140.19, 139.38, 136.57, 136.36, 133.53, 128.39, 128.04, 126.84, 126.35, 123.97, 121.58, 121.22, 120.26, 71.10, 70.39, 70.00, 67.28, 55.38, 51.67, 40.21, 34.03, 32.65, 30.13, 29.09, 27.78, 24.95, 23.73. Elemental analysis calcd (%) for C_{42.3}H_{48.8}Br_{3.2}O_{2.4}N_{0.8}S_{0.4}: C 58.04, H 5.62, N 1.28. Found: C 57.92, H 5.69, N 1.15.

Synthesis of P1. Condensed trimethylamine (2 mL) was added dropwise to a solution of **P0** (50 mg) in THF (10 mL) at –78 °C. The mixture was allowed to warm to room temperature. The precipitate

was redissolved by the addition of water (10 mL). After the mixture was cooled to –78 °C, additional trimethylamine (2 mL) was added, and the mixture was stirred at room temperature for 24 h. After solvent removal, acetone was added to precipitate **P1** (55 mg) as an orange glassy solid in 85% yield. ¹H NMR (400 MHz, CD₃OD, δ ppm): 8.33–7.76 (m, 10.4 H), 3.82–3.73 (br, 2.40 H), 3.55–3.40 (m, 4.80 H), 3.14–3.00 (m, 28.8 H), 2.88–2.18 (m, 4.80 H), 1.68–1.56 (br, 4 H), 1.39–1.20 (br, 8 H), 1.15–0.66 (br, 4 H). ¹³C NMR (100 MHz, CD₃OD, δ ppm): 155.62, 153.60, 153.02, 152.30, 151.79, 151.06, 142.53, 141.84, 141.14, 140.44, 138.04, 137.81, 134.47, 133.22, 131.74, 129.80, 127.99, 127.51, 126.13, 125.23, 122.80, 122.44, 121.71, 71.44, 70.79, 68.56, 68.37, 67.75, 66.95, 65.92, 56.80, 54.90, 53.62, 41.22, 30.35, 26.96, 25.05, 23.72.

Acknowledgment. The authors are grateful to the National University of Singapore (ARF R-279-000-197-112/133, R-279-000-233-123 and YIA R-279-000-234-123) and Singapore Ministry of Education (R-279-000-255-112) for financial support.

References and Notes

- (1) (a) Capila, I.; Linhardt, R. J. *Angew. Chem., Int. Ed.* **2002**, *41*, 390–412. (b) Whitelock, J. M.; Iozzo, R. V. *Chem. Rev.* **2005**, *105*, 2745–2764.
- (2) (a) Linhardt, R. J.; Gunay, N. S. *Semin. Thromb. Hemostasis* **1999**, *25*, 5–16. (b) Fareed, J.; Hoppensteadt, D. A.; Bick, R. L. *Semin. Thromb. Hemostasis* **2000**, *26*, 5–21.
- (3) (a) Freedman, M. D. *J. Clin. Pharmacol.* **1992**, *32*, 584–596. (b) Wallis, D. E.; Lewis, B. E.; Messmore, H.; Wehrmacher, W. H. *Clin. Appl. Thromb. Hemostasis* **1998**, *4*, 160–163. (c) Walenga, J. M.; Bick, R. L. *Med. Clin. North Am.* **1998**, *82*, 635–648.
- (4) Raymond, P. D.; Ray, M. J.; Callen, S. N.; Marsh, N. A. *Perfusion* **2003**, *18*, 269–276.
- (5) Boneu, B.; de Moerloose, P. *Semin. Thromb. Hemost.* **2001**, *27*, 519–522.
- (6) (a) Kitchen, S. *Br. J. Haematol.* **2000**, *111*, 397–406. (b) Levine, M. N.; Hirsh, J.; Gent, M.; Turpie, A. G.; Cruickshank, M.; Weitz, J.; Anderson, D.; Johnson, M. *Arch. Int. Med.* **1994**, *154*, 49–56.
- (7) (a) Zhong, Z.; Anslyn, E. V. *J. Am. Chem. Soc.* **2002**, *124*, 9014–9015. (b) Wright, A. T.; Zhong, Z.; Anslyn, E. V. *Angew. Chem., Int. Ed.* **2005**, *44*, 5679–5682. (c) Sun, W.; Bandmann, H.; Schrader, T. *Chem.—Eur. J.* **2007**, *13*, 7701–7707.
- (8) Saucedo, J. C.; Duke, R. M.; Nitz, M. *ChemBioChem* **2007**, *8*, 391–394.
- (9) (a) Chen, L.; McBranch, D. W.; Wang, H. L.; Helgeson, R.; Wudl, F.; Whitten, D. G. *Proc. Natl. Acad. Sci. U.S.A.* **1999**, *96*, 12287–12292. (b) Peter, K.; Nilsson, R.; Inganäs, O. *Nat. Mater.* **2003**, *2*, 419–424. (c) Liu, B.; Bazan, G. C. *Chem. Mater.* **2004**, *16*, 4467–4476. (d) Haskins-Glusac, K.; Pinto, M. R.; Tan, C.; Schanze, K. S. *J. Am. Chem. Soc.* **2004**, *126*, 14964–14971. (e) Ho, H. A.; Béra-Abérend, M.; Leclerc, M. *Chem.—Eur. J.* **2005**, *11*, 1718–1724. (f) Miranda, O. R.; You, C. C.; Phillips, R.; Kim, I. B.; Ghosh, P. S.; Bunz, U. H. F.; Rotello, V. M. *J. Am. Chem. Soc.* **2007**, *129*, 9856–9857. (g) Bazan, G. C. *J. Org. Chem.* **2007**, *72*, 8615–8635.
- (10) Thomas, S. W., III; Joly, G. D.; Swager, T. M. *Chem. Rev.* **2007**, *107*, 1339–1380.
- (11) (a) Schwartz, B. *J. Annu. Rev. Phys. Chem.* **2003**, *54*, 141–172. (b) Hennebicq, E.; Pourtois, G.; Scholes, G. D.; Herz, L. M.; Russell, D. M.; Silva, C.; Setayesh, S.; Grimdale, A. C.; Müllen, K.; Brédas, J. L.; Beljonne, D. *J. Am. Soc. Chem.* **2005**, *127*, 4744–4762. (c) Praveen, V. K.; George, S. J.; Varghese, R.; Vijayakumar, C.; Ajayaghosh, A. *J. Am. Soc. Chem.* **2006**, *128*, 7542–7550.
- (12) Liu, B.; Bazan, G. C. *J. Am. Chem. Soc.* **2004**, *126*, 1942–1943.
- (13) (a) Hong, J. W.; Hemme, W. L.; Keller, G. E.; Rinke, M. T.; Bazan, G. C. *Adv. Mater.* **2006**, *18*, 878–882. (b) Chi, C.; Mikhailovsky, A.; Bazan, G. C. *J. Am. Chem. Soc.* **2007**, *129*, 11134–11145.
- (14) Satrijo, A.; Swager, T. M. *J. Am. Chem. Soc.* **2007**, *129*, 16020–16028.
- (15) Yu, D.; Zhang, Y.; Liu, B. *Macromolecules* **2008**, *41*, 4003–4011.
- (16) Pu, K. Y.; Fang, Z.; Liu, B. *Adv. Funct. Mater.* **2008**, *18*, 1321–1328.
- (17) [RU] has a molecular weight of 1065.7 g/mol, which includes 1 mol of (trimethylammonium)hexyl-substituted fluorene, 0.6 mol of (trimethylammonium)ethoxyethoxyethyl-substituted fluorene, and 0.4 mol of BT.
- (18) Hirsh, J.; Raschke, R. *Chem* **2004**, *126*, 188–203.
- (19) Liu, B.; Bazan, G. C. *Nat. Protoc.* **2006**, *1*, 1698–1702.
- (20) Keana, J. F. W.; Wu, Y.; Wu, G. *J. Org. Chem.* **1987**, *52*, 2571–2576.